Chemico-Biological Interactions 372 (2023) 110357

Contents lists available at ScienceDirect

Chemico-Biological Interactions

journal homepage: www.elsevier.com/locate/chembioint

Research paper

# Antioxidant activity and enzymatic of lichen substances: A study based on cyclic voltammetry and theoretical

Osvaldo Yañez [a,b], Manuel I. Osorio [c,d], Edison Osorio [e], William Tiznado [f], Lina Ruíz [g], Camilo García [h], Orlando Nagles [i], Mario J. Simirgiotis [j], Grover Castañeta [k], Carlos Areche [k,**], Olimpo García-Beltrán [e,l,*]

[a] Facultad de Ingeniería y Negocios, Universidad de las Américas, Santiago, 7500000, Chile
[b] Center of New Drugs for Hypertension (CENDHY), Santiago, 8380494, Chile
[c] Center for Bioinformatics and Integrative Biology (CBIB), Facultad de Ciencias de la Vida, Universidad Andres Bello, Av. República 330, Santiago, 8370146, Chile
[d] Facultad de Medicina, Centro de Investigación Biomédica, Universidad Diego Portales, Ejército 141, Santiago, 837007, Chile
[e] Facultad de Ciencias Naturales y Matemáticas, Universidad de Ibagué, Carrera 22 Calle 67, Ibagué, 730002, Colombia
[f] Facultad de Ciencias Exactas, Departamento de Ciencias Químicas, Universidad Andrés Bello, Avenida República 275, Piso 3, Santiago, Chile
[g] Centro de Investigación Biomédica, Universidad Autónoma de Chile, Santiago, Chile
[h] Universidad Católica de Temuco, Facultad de Recursos Naturales, Departamento de Ciencias Biológicas y Químicas, Avenida Rudecindo Ortega, 02950, Campus San Juan Pablo II, Temuco, Chile
[i] Facultad de Química e Ingeniería, Universidad Nacional Mayor de San Marcos, Lima, Peru
[j] Instituto de Farmacia, Facultad de Ciencias, Universidad Austral de Chile, Campus Isla Teja, Valdivia, 5090000, Chile
[k] Departamento de Química, Facultad de Ciencias, Universidad de Chile, Santiago, Chile
[l] Centro Integrativo de Biología y Química Aplicada (CIBQA), Universidad Bernardo O'Higgins, General Gana 1702, Santiago, 8370854, Chile

ARTICLE INFO

*Keywords:*
Lichenic substances
Antioxidant
Cyclic voltamperograms
DFT methods
CYPs enzymes
Natural products

ABSTRACT

The antioxidant activity of nine lichen substances, including methylatrarate (1), methyl haematommate (2), lobaric acid (3), fumarprotocetraric acid (4), sphaerophorin (5), subsphaeric acid (6), diffractaic acid (7), barbatolic acid (8) and salazinic acid (9) has been determined through cyclic voltammetry. The compounds 1–4 presented slopes close to the Nernst constant of 0.059 V, indicating a $2H^+/2e^-$ relation between protons and electrons, as long as the compounds 5, 6, 7, 8, and 9 present slopes between 0.037 V and 0.032 V, indicating a $1H^+/2e^-$ relation between protons and electrons. These results show a high free radical scavenging activity by means of the release of $H^+$, suggesting an important antioxidant capacity of these molecules. Theoretical calculations of hydrogen bond dissociation enthalpies (BDE), proton affinities (PA), and Proton Transfer (PT) mechanisms, at M06-2x/6-311+G(d,p) level complement the experimental results. Computations support that the best antioxidant activity is obtained for the molecules (3, 4, 5, 6, 7 and 8), that have a carboxylic acid group close to a phenolic hydroxyl group, through hydrogen atomic transfer (HAT) and sequential proton loss electron transfer (SPLET) mechanisms. Additional computations were performed for modelling binding affinity of the lichen substances with CYPs enzymes, mainly CYP1A2, CYP51, and CYP2C9*2 isoforms, showing strong affinity for all the compounds described in this study.

## 1. Introduction

The natural antioxidants can protect the human body from reactive oxygen species (ROS) or oxidative stress [1], which is an imbalance between the production of reactive species and antioxidant defense activity [2]. These ROS species are a known contributing factor to many chronic diseases such as cancer, diabetes, neurodegenerative and cardiovascular diseases [3]. The production of ROS is a natural by-product of several essential biochemical reactions, in special the mitochondrial electron transport chain, generally regulated by the presence of antioxidants [4].

Lichens are symbiotic associations between a fungus and one or more

* Corresponding author. Facultad de Ciencias Naturales y Matemáticas, Universidad de Ibagué, Carrera 22 Calle 67, Ibagué, 730002, Colombia.
** Corresponding author.
*E-mail addresses:* areche@uchile.cl (C. Areche), jose.garcia@unibague.edu.co (O. García-Beltrán).

https://doi.org/10.1016/j.cbi.2023.110357
Received 30 August 2022; Received in revised form 11 January 2023; Accepted 20 January 2023
Available online 21 January 2023

photosynthetic organisms (green algae or a cyanobacterium), resulting in a morphologically different thallus to each of its components as a totally new morphological entity [5]. These species are used in traditional medicine and they are rich in secondary metabolites, known as lichenic substances (depsides, depsidones, dibenzofurans, pulvinic acid derivatives) and pigments (anthraquinones, napthoquinones, and xanthones) which are bioactive compounds that have shown widespread use [6–13].

Lichens evolved in a wide variety of ecosystems, favoring the creation of a wide variety of lichenic substances, this has allowed knowing multiple biological activities, being the most outstanding the enzymatic inhibition activities of cholinesterase, inhibitors of SARS-CoV-2 3CL Protease, antimycobacterial activity against multidrug-resistant tuberculosis strains, anthelmintic, cytotoxic and antioxidant activity [11, 14–21]. Lichens biosynthesize substances' high antioxidant activity, attributed to the number of hydroxyl (OH) groups present in their aromatic ring(s) [22]. The theoretical analysis of phenolic molecules is an important field because it allows us to understand and determine the mechanism of radical scavenging, and common motifs, involved in the antioxidant activity helping in the rational design of novel antioxidants [23]. In this context, the antioxidant properties of lichen substances measured by voltammetry and associated with computational approaches based on hydrogen atom transfer (HAT) [24] and sequential proton loss electron transfer (SPLET) [25] mechanisms are necessary for expanding our knowledge about the radical scavenger capability of these phenolic compounds. Some of the authors of this work showed the importance of theoretical studies to provide insight into important aspects of the mechanisms and antioxidant activities of different polyphenolic compounds [26–28] about the antioxidant activity in lichen substances and only few computational works (add references). Herein we evaluate the antioxidant activity of nine lichen substances by analyzing cyclic voltammetry measurements and theoretical calculations: computed thermochemical properties using DFT methods and molecular docking for exploring possible antioxidant activity mediated by Cytochrome P450 (CYP) enzymes by estimating the affinity of the lichen compounds for CYPs enzyme isoforms. The latter analysis suggests that the isoform with the highest affinity for the majority for the compounds is CYP2C9*2.

## 2. Methods

### 2.1. Materials

Species of *Umbilicaria antarctica* Frey & I.M. Lamb, *Cladonia metacorallifera, Sphaerophorus globosus*, *Coelopogon epiphorellum,* and *Himantormia lugubris* were collected in "Peninsula Fildes", King George Island, Antarctic, March of, 2019. Samples were identified and vouchers specimens were deposited at the Extreme Natural Product Laboratory, Universidad de Chile with the reference numbers: UA-010414, CM-010414, SG-010414, CE-010414, and HL-010414 respectively. *Stereocaulon glareosum* and *Usnea barbata*, were collected at Huaraz - Perú, in 2013 and at Chillan, VIII Region-Chile, in 2015. A voucher specimen Nº ST-10062013 and UB-06092015 was generated, respectively.

### 2.2. Extraction and isolation

The dried lichen species were extracted with MeOH (Sigma Aldrich Co., Santiago, Chile) and the extracts obtained were purified first by Sephadex LH-20 (MeOH as mobile phase) (Sigma Aldrich Co., Santiago, Chile) and further by column chromatography (CC), Silica gel ($SiO_2$) (Kieselgel 60, Merck, Santiago, Chile 0.063–0.200 mm). All compounds were identified by comparing the $^1$H NMR spectra (Avance II 400 MHz multidimensional spectrometer, Bruker Corporation, Billerica, MA, USA) with those of scientific literature (Huneck and Yoshimura 1996).

*Everniosis trulla* (30 g) afforded 30 mg methylatrarate (**1**) and 45 mg methyl haematommate (**2**), while *Umbilicaria antarctica* (50 g) gave 120 mg lobaric acid (**3**) [29]. Fumarprotocetraric acid (25 mg;**4**) was isolated from *Cladonia cariosa* (25 g) [30], while sphaerophorin (44 mg; **5**) and subsphaeric acid (68 mg; **6**) from *Sphaerophorus globosus* (10 g) and *Coelopogon epiphorellum* (15 g), respectively. Finally, *Usnea barbata* (100 g) and *Himantormia lugubris* (30 g) afforded the compounds diffractaic acid (119 mg; **7**) [29], barbatolic acid (98 mg; 8) [30]. and salazinic acid (19 mg; **9**) [29].

### 2.3. Measurement procedure for cyclic voltammetry

The electrochemical cell was constituted by a system of three incorporated screen-printed electrodes (DRP C110, DRP-110 SWCNT DropSens, Oviedo, Spain) with a working electrode of carbon (4 mm), Ag pseudo reference electrode and carbon as counter electrode. 3.0 mg of sample were dissolved in 0.1 mL of 0.01 M PBS (Merck Co., Bogotá, Colombia). 0.05 mL of the dissolved sample was deposited on the screen-printed surface of the electrodes. After 5 s the voltammograms were scanned from 0.0 to 1.2 V with scan rate 0.05 $Vs^{-1}$.

### 2.4. Theoretical approaches and computational details

All optimizations and frequency calculations for the neutral, radicals, and cations conformations were performed at M06-2X [31]/6-311+G(d, p) [32,33] level, using the Gaussian 16 software [34]. The water solvent was considered through the implicit polarizable continuous model (PCM) formalism. Complete explorations of the intramolecular interactions were taken into account to choose the most stable geometries. Finally, frequency calculations analysis verified that all the structures studied are true minima on the potential energy surface (PES).

To determine the mechanistic pathway of the radical scavenging process, thermochemical properties were used by assessing the energetics of the determining step of each pathway. The literature recognizes three common mechanisms of antioxidant activity. The first corresponds to the hydrogen atom transfer (HAT), regularly used for gas-phase reactions. The leader step corresponds to homolytic bond breakage as an appropriate moiety to yield a hydrogen radical ($H^{\bullet}$), followed by reactions with free-radical ($R^{\bullet}$) species.

$$R-H \rightarrow R^{\bullet} + H^{\bullet}(BDE) \quad (1)$$

The antioxidant capacity is assessed by the R–H moiety's lowest bond dissociation enthalpy (BDE). The second mechanism corresponds to a single electron transfer followed by a proton transfer (SET-PT) [35], where the initial step corresponds to electron ($e^{-}$) loss to form a radical cation ($RH^{+\bullet}$) followed by a deprotonating step.

$$R-H \rightarrow RH^{+\bullet} + e^{-}\ (IE) \quad (2)$$

$$RH^{+\bullet} \rightarrow R^{\bullet} + H^{+}(PDE) \quad (3)$$

The lowest ionization energy (IE) value for the first step and the proton dissociation enthalpy (PDE) for the second step should determine the facility as an antioxidant molecule. Finally, the third mechanism corresponds to the sequential proton loss electron transfer (SPLET). This turns into a dissociation of an acidic moiety, which can be characterized by proton affinity (PA). The lowest PA values establish an important step for the antioxidant activity; subsequently, an electron transfer follows the reaction to the free radical at the cost of the electron transfer energy (ETE)

$$R-H \rightarrow R^{-} + H^{+}(PA) \quad (4)$$

$$R^{-} \rightarrow R^{\bullet} + e^{-}(ETE) \quad (5)$$

Consequently, the reaction enthalpies (H) of the individual steps in the mechanisms of the antioxidant activity described above in the gas phase (at 298.15 K and 1 atm) are calculated as follows:

$$BDE = H(R^{\bullet}) + H(H^{\bullet}) - H(R-H) \quad (6)$$

$$IE = H(RH^{\bullet+}) + H(e^{-}) - H(R-H) \quad (7)$$

$$PDE = H(R^{\bullet}) + H(H^{+} - H(R^{\bullet+}) \quad (8)$$

$$PA = H(R^{-}) + H(H^{+}) - H(R-H) \quad (9)$$

$$ETE = H(R^{\bullet}) + H(e^{-}) - H(R^{-}) \quad (10)$$

The standard values of the enthalpies for electron and proton in the gas phase can be taken from the commonly accepted values of 0.002360 Hartree (6.197 kJ/mol) for the proton enthalpy and 0.001200 Hartree (3.146 kJ/mol) for the electron enthalpy [36].

### 2.5. Docking and ligand efficiency approach

Computational modelling of the interaction of the lichen species with **CYP1A2** (PDB Code: 2HI4) [37], **CYP51** (PDB Code: 5FSA) [38], **CYP2C9*2** (PDB Code: 6VLT) [39] and **CYP134A1** (PDB Code: 7OW9) [40] proteins was performed, were downloaded from the Protein Data Bank [41]. AutoDock Vina (v1.0.2) [42] was used for all dockings in this study. The three-dimensional coordinates of all structures were optimized using MOPAC2016 [43] software by PM6-D3H4 semi-empirical method [44,45]. The ligand files were prepared using the Open Source Chemistry Toolbox, Open Babel suite [46]. The Mulliken partial atomic charges of each ligand were determined with the PM6-D3H4 semi--empirical method; this approach introduces dispersion and hydrogen-bonded corrections to the PM6 method. All CYP proteins were treated with Schrödinger's Protein Preparation Wizard [47]; polar hydrogen atoms were added, nonpolar hydrogen atoms were merged, and charges were assigned. Docking was treated as rigid and carried out using the empirical free energy function and the Lamarckian Genetic Algorithm provided by AutoDock Vina [48]. The grid map dimensions were 20 × 20 × 20 $Å^3$, making the binding pocket of **CYP1A2** the center coordinates 6.308, 21.274 and 21.356, the binding pocket of **CYP51** was defined the centre coordinates 194.870, −4.531 and 36.296, the binding pocket of **CYP2C9*2** was defined the centre coordinates 35.058, 42.073 and −4.100, and the binding pocket of **CYP134A1** was defined the centre coordinates −18.056, −4.676 and −18.457. All other parameters were set as the default defined by AutoDock Vina. Dockings were repeated 50 times with space search exhaustiveness set to 100. The best interaction binding energy (kcal·$mol^{-1}$) was selected for evaluation. Docking results 3D representations were used Discovery Studio [49] 3.1 (Accelrys, CA) molecular graphics system. Furthermore, the non-covalent interaction index (NCI) [50,51] was used to qualitatively identify the areas where intermolecular such as hydrogen bonds, steric repulsion, and Van der Waals interactions predominate in the structural protein-ligand. All calculations were performed with NCIPlot software and Molecular visualization of the systems was carried out with the VMD software package [52].

Ligand efficiency (LE) calculations were performed using one parameter $K_d$. The $K_d$ parameter corresponds to the dissociation constant between a ligand/protein, and their value indicates the bond strength between the ligand/protein [53–55]. $K_d$ calculations were done using the following equations:

$$K_d = 10^{\frac{\Delta G^0}{2.303RT}} \quad (1)$$

where $\Delta G^0$ is the binding energy (kcal·$mol^{-1}$) obtained from docking experiments, R is the gas constant, and T is the temperature in Kelvin. The LE allows us to compare molecules according to their average binding energy [55,56]. Thus, it determined as the ratio of binding energy per non-hydrogen atom, as follows [53–55,57]:

$$LE = -\frac{2.303RT}{HAC}\log(K_d) \quad (2)$$

where $K_d$ is obtained from equation (1) and HAC denotes the heavy atom count (i.e., number of non-hydrogen atoms) in a ligand. Binding Efficiency Index (BEI), and Lipophilic Ligand Efficiency (LLE) are calculated based on the $K_d$ obtained from molecular docking. BEI allows to estimate the binding capacity weighted by the molar mass (equation (3)), whereas LLE (equation (4)) estimates the binding capacity concerning its lipophilicity (clogP obtained from SwissADME webserver) [58,59].

$$BEI = \frac{-log(K_d)}{MW} \quad (3)$$

$$LLE = -log(K_d) - clogP \quad (4)$$

## 3. Results and discussion

From methanolic extracts of lichen species and after repeated column chromatography, the following compounds were isolated: methylatrarate (**1**) and methyl haematommate (**2**) from *Everniopsis trulla*, lobaric acid (**3**) from *Umbilicaria Antarctica;* fumarprotocetraric acid (**4**) from *Cladonia cariosa*, Sphaerophorin (**5**)from *Sphaerophorus globosus*, subsphaeric acid (**6**) from *Coelopogon epiphorellum*, diffractaic acid (**7**) and salazinic acid (**9**) from *Usnea barbata*, and barbatolic acid (**8**) from *Himantormia lugubris* (Fig. 1).

Cyclic voltammetry of every lichen extract shows irreversible oxidation attributable to the phenolic component present in structures 1 to 9. In the case of methylatrarate (**1**) 1, two irreversible waves can be observed associated with second oxidation at a pH higher than 6.90. Toward pH values lower than 6.90, only one peak oxidation can be observed, where only one process is observed. Similar behavior is present for subsphaeric acid (**6**) and diffractaic acid (**7**). On the other hand, methylhaeatommate (2) showed only one oxidation process in all the pH ranges studied.

Through cyclic voltamperograms experiments, linear regression equations between peak potential as pH function were constructed to understand the electrochemical behavior of these lichen substances and relate those results with the Nernst slope (0.059 V/n, where n = electron consumed for the electrochemical process), Table 1. The negative signs in the slope or gradient (m) values indicate that as the pH increases, the reduction potentials are moving to lower negative values, demonstrating that in all lichen molecules, the oxidation involves $H^+$ protons and requires low oxidation energy at higher pH values. Those results are similar to other substances with antioxidant activity, such as polyphenols and vitamins [60].

The electrochemistry measurements provide interesting results: lichens molecules1-4 (Supporting Information Figs. S1 and S2)(Fig. 2) presented slopes close to the Nernst constant, 0.059 V/pH, indicating a $2H^+/2e^-$ relation between protons and electrons. On the other hand, the 5–9 systems with slopes between 0.037 V/pH and 0.032 V/pH indicated a $1H^+/2e^-$ relation between protons and electrons (Supporting Information Figs. S3–S7). These results show that the oxidation process of these lichen molecules is a process where $H^+$ is released (Apak 2018). On the other hand, the shift of less positive potential values can improve the antioxidant activity in alkaline media of these substances because they require less energy to oxidize. An anodic peak current can be related to the antioxidant concentration from the extract [61]. In this report, all lichenic compounds showed near current values and, in some cases, greater than 100 μAA.

Previous studies showed that the BDE value is an important descriptor in evaluating compounds' antioxidant activity as it characterizes the ability to donate hydrogen radical and form a stable radical of the donor. According to this idea, the theoretical antioxidant activity of three natural compounds derived from lichens, such as atranorin (AT), evernico acid (EV), and diffractic acid (DF), have been carried out examining the main mechanisms for the antioxidant action of polyphenols [31]. In this study, the hydrogen atom transfer (HAT) (Burton et al., 1985) and sequential proton loss electron transfer (SPLET) [25] mechanisms are the most conceivable for the antioxidant action of this

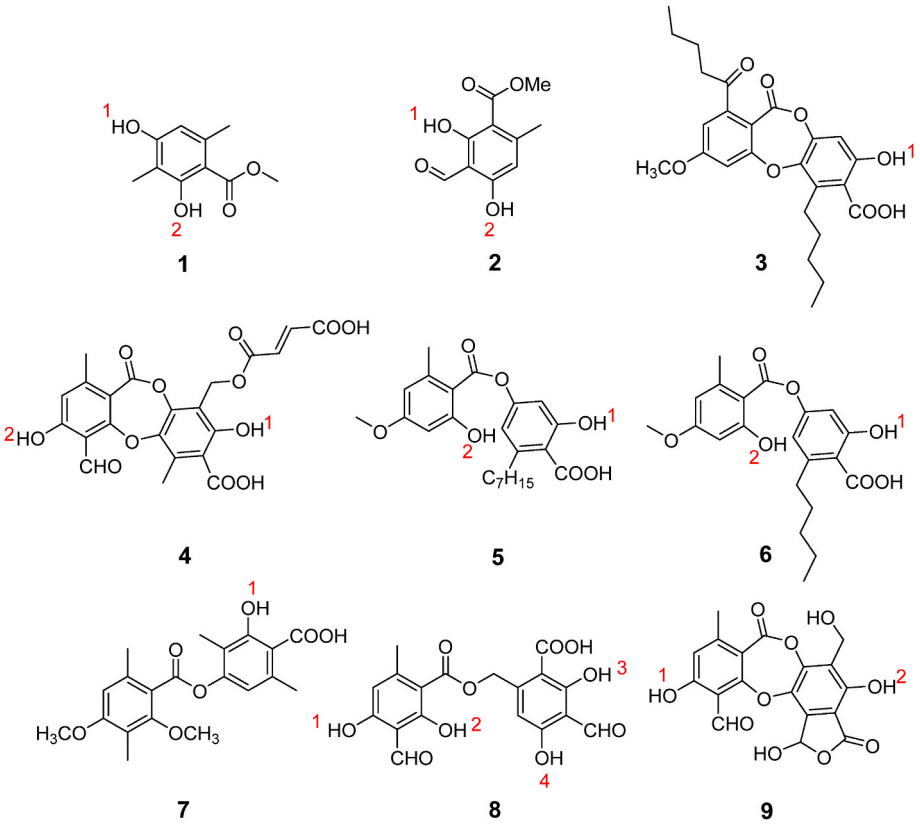


**Fig. 1.** Isolated compounds and analyzed in this work, indicate the H atoms.

**Table 1**
Linear regression equations, $E_{pa}(V) = a + mpH$, for purified lichen substances as function of pH.

| | Name Molecule | a | m | $R^2$ | RSD |
|---|---|---|---|---|---|
| **1** | Methylatrarate | 0.952 | - 0.069 | −0.98 | 0.039 |
| **2** | Methylhaeatommate | 0.923 | - 0.066 | −0.97 | 0.052 |
| **3** | Lobaric acid | 0.988 | - 0.058 | −0.99 | 0.013 |
| **4** | Fumarprotocetraric acid | 0.879 | - 0.051 | −0.97 | 0.040 |
| **5** | Sphaeroforin | 0.791 | - 0.037 | −0.99 | 0.015 |
| **6** | Subsphaeric acid | 0.827 | - 0.035 | −0.93 | 0.049 |
| **7** | Diffractaic acid | 0.775 | - 0.036 | −0.98 | 0.03 |
| **8** | Barbatolic acid | 0.654 | - 0.032 | −0.92 | 0.049 |
| **9** | Salazinic acid | 0.868 | - 0.032 | −0.99 | 0.009 |

class of compounds. In a HAT mechanism, the BDE value predicts the susceptibility of the antioxidant molecule to donate a hydrogen atom and form a radical. So, a lower value of the O–H bond corresponds to a higher antioxidant capacity. The BDEs values for the phenolic ArO-H hydroxyl bonds are reported in Table 2 (Fig. 1).

According with the results in Table 2, the 5 and 6 lichenic molecules have the lowest BDEs. Both systems have the same values due to they only differ in the length of the aliphatic chain, which is not involved in the direct antioxidant process. The high stability of these radical species is due to the presence of intramolecular hydrogen bonds formed between the radical oxygen and the hydrogen atom of the carboxyl group located contiguous to the phenolic Ar-OH hydroxyl (see Fig. 3). Moreover, 5 and 6 molecules presented anodic peak currents, higher than 0.150 mA, and are oxidized to a potential greater than 0.4 V at pH values between 6.0 and 10.0 indicating a greater rate in the transfer of charge and high stability compared with the other lichenic substances. Similarly, these interactions are responsible to stabilize the 3, 4, 7, and 8 radical systems. In the case of 9, the intramolecular hydrogen bond is formed between the radical oxygen and a hydroxyl group. These results indicate that a carboxylic acid group close to a phenolic hydroxyl plays an important role in the antioxidant mechanism, stabilizing the radical form. In the case of 1 and 2 lichenic molecules, both radicals are stabilized only by the electron density delocalization on the aromatic ring.

For the second antioxidant mechanism analyzed, SETPT, a lower IE means a higher antioxidant activity. The ionization enthalpies (IE) and the proton dissociation enthalpies (PDE) for the phenolic hydroxyl bonds are presented in Table 3.

According to the antioxidant activity of these molecules (Table 3), there are three groups: the first involves 1 and 7, with IEs values between 122 and 123 kcal $mol^{-1}$; in the second group are 3, 5 and 6, with values of 127 kcal $mol^{-1}$ and finally the 2, 4, 8 and 9 systems, which have IE values between 130 and 132 kcal $mol^{-1}$. In the case of PDEs values, the radical molecules formed in the second step show values located between 247 and 260 kcal $mol^{-1}$, where 5 and 6 present the lowest values while 1, 7, and 8 have the highest. In general terms, all molecules are phenolic and there is no significant structural difference between them to explain the differences in the ionization enthalpies, so we can conclude that this mechanism is not the most adequate to explain the antioxidant activity of lichen substances studied.

Finally, in the sequential proton loss electron transfer (SPLET) mechanism the antioxidant activity begins with the dissociation of acid and is characterized by the proton affinity (PA), consequently, a low value is characteristic of a higher antioxidant capacity. The antioxidant mechanism continues with the transfer of an electron to a free radical at a cost of electron transfer energy (ETEs). In Table 4 the PAs and PDEs for the phenolic hydroxyl bonds are presented.

According to the results presented in Table 4, the 4, 5, and 6 molecules have the lowest PA values, from 271 to 273 kcal $mol^{-1}$. Moreover, according to the structural similarity of the lichenic molecules, the 3, 7, and 8 conformations can be associated with the same group. Just like the HAT mechanism, the most stable anionic species are formed from the phenolic hydroxyl groups that are close to an acid carboxylic group. In

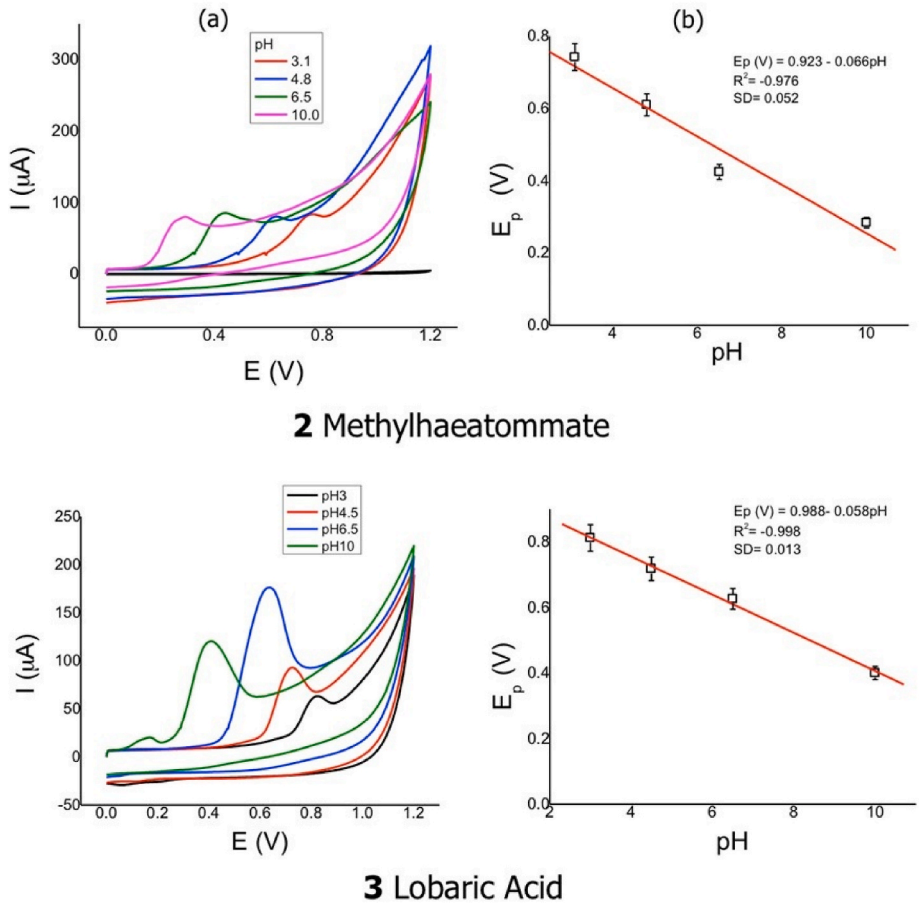


**Fig. 2.** Cyclic voltamperograms and linear regression as pH function for ethylhaeatommate (2) and lobaric acid (3).

**Table 2**
Calculated BDEs values for the phenolic Ar-OH hydroxyl bonds associated with the HAT mechanism.

| | Lichen substances | Ar-OH position | BDE (kcal.mol$^{-1}$) |
|---|---|---|---|
| **1** | Methylatrarate | O1–H | 89.5 |
| | | O2–H | 92.8 |
| **2** | Methylhaeatommate | O1–H | 100.5 |
| | | O2–H | 92.9 |
| **3** | Lobaric acid | O1–H | 92.9 |
| **4** | Fumarprotocetraric acid | O1–H | 93.4 |
| | | O2–H | 100.6 |
| **5** | Sphaeroforin | O1–H | 90.1 |
| | | O2–H | 85.6 |
| **6** | Subsphaeric acid | O1–H | 90.1 |
| | | O2–H | 85.6 |
| **7** | Diffractaic acid | O1–H | 93.1 |
| **8** | Barbatolic acid | O1–H | 101.7 |
| | | O2–H | 96.3 |
| | | O3–H | 96.4 |
| | | O4–H | 103.0 |
| **9** | Salazinic acid | O1–H | 104.7 |
| | | O2–H | 92.6 |

the case of 9, the anionic species are stabilized by the presence of two hydrogen bonds formed with an aldehyde and a hydroxyl group. However, the difference in ETEs, 139.8 *vs* 127.6 kcal mol$^{-1}$, show that the radical specie is more stable in the presence of the hydrogen bond formed with the other OH group.

Finally, isosurfaces of the spin density for the lichens in the second step of the sequential proton loss electron transfer (SPLET) mechanism (Fig. 4), show that all molecules present an electron delocalization on the aromatic ring.

All theoretical results indicate to 5 and 6 as lichenic substances with more antioxidant activity. Up to this point, the electrochemical study shows that the antioxidant capacity does not depend on the number of protons and electrons involved in the oxidation process and on the contrary is related to the stability and proton capacity (PA) that the theoretical and electrochemical studies up to this point coincide with 5 and 6.

To estimate and evaluate the affinity of the molecules for the CYPs isoforms, in order to form a highly stable complex, free energy calculations were performed by molecular docking, and the ligand efficiency was determined for each of the lichenic compounds. The interaction of the lichenic compounds with CYPs could generate a decrease in the oxidative potential by inhibition of CYPs or by the activity of the lichenic compounds after being processed by the same CYPs. To evaluate the affinity for CYPs, the binding free energy of the lichenic compounds and four crystallized CYP isoforms was calculated (Fig. 5). As shown in Fig. 5, the binding free energy of less than −4.0 kcal/mol was obtained for the CYP isoforms studied. However, CYP1A and CYP2C9*2 binding energy is lower than −6.4 kcal mol$^{-1}$.

To avoid over estimation due to the size of the molecules, *LE* was calculated. From these calculations it is observed that the compounds methylatrarate and methylhaeatommate have a high binding efficiency with CYP1A2, CYP51 and CYP2C9*2 (Fig. 6). In contrast, lobaric acid and fumarprotocetraric acid have high binding efficiency with CYP1A2, CYP51 and CYP2C9*2. The compound methylatrarate is the only one with a high affinity for the CYP134A1 isoform.

CYP2C9 is one of the isoenzymes with the highest affinity for lichenic compounds and is responsible for the highest metabolic capacity of the CYP family [62]. To evaluate the affinity of lichenic compounds for this

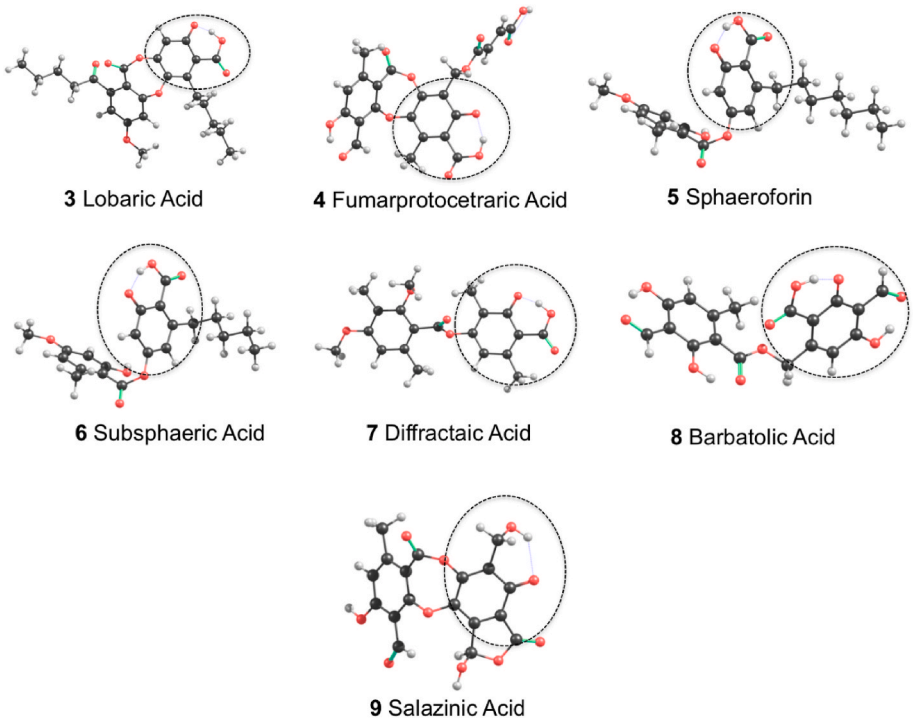


**Fig. 3.** Most stable species and their stabilizing intramolecular hydrogen bonds.

**Table 3**
Calculated IEs and PDEs for the phenolic Ar-OH hydroxyl bonds associated to SETPT mechanism.

| | Lichen substances | IE (kcal. $mol^{-1}$) | Ar-OH position | PDE (kcal. $mol^{-1}$) |
|---|---|---|---|---|
| **1** | Methylatrarate | 122.3 | O1–H | 255.5 |
| | | | O2–H | 258.8 |
| **2** | Methylhaeatommate | 130.3 | O1–H | 258.5 |
| | | | O2–H | 250.9 |
| **3** | Lobaric acid | 127.2 | O1–H | 253.9 |
| **4** | Fumarprotocetraric acid | 129.9 | O1–H | 251.7 |
| | | | O2–H | 258.9 |
| **5** | Sphaeroforin | 126.9 | O1–H | 251.5 |
| | | | O2–H | 247.0 |
| **6** | Subsphaeric acid | 126.7 | O1–H | 251.8 |
| | | | O2–H | 247.2 |
| **7** | Diffractaic acid | 123.4 | O1–H | 257.9 |
| **8** | Barbatolic acid | 130.4 | O1–H | 259.5 |
| | | | O2–H | 254.1 |
| | | | O3–H | 254.2 |
| | | | O4–H | 260.8 |
| **9** | Salazinic acid | 132.1 | O1–H | 260.9 |
| | | | O2–H | 248.8 |

**Table 4**
Calculated PAs and ETEs for the phenolic Ar-OH hydroxyl bonds associated with SETPT mechanism.

| | Lichen substances | Ar-OH position | PAs (kcal. $mol^{-1}$) | ETEs (kcal. $mol^{-1}$) |
|---|---|---|---|---|
| **1** | Methylatrarate | O1–H | 287.4 | 115.5 |
| | | O2–H | 296.1 | 110.1 |
| **2** | Methylhaeatommate | O1–H | 288.9 | 124.9 |
| | | O2–H | 280.3 | 125.9 |
| **3** | Lobaric acid | O1–H | 290.3 | 115.9 |
| **4** | Fumarprotocetraric acid | O1–H | 273.2 | 133.5 |
| | | O2–H | 285.3 | 128.7 |
| **5** | Sphaeroforin | O1–H | 286.9 | 116,6 |
| | | O2–H | 271.4 | 127.6 |
| **6** | Subsphaeric acid | O1–H | 286.9 | 116,7 |
| | | O2–H | 271.2 | 127.7 |
| **7** | Diffractaic acid | O1–H | 293.3 | 113.2 |
| **8** | Barbatolic acid | O1–H | 287.9 | 127.2 |
| | | O2–H | 287.4 | 122.3 |
| | | O3–H | 284.1 | 125.7 |
| | | O4–H | 284.7 | 131.7 |
| **9** | Salazinic acid | O1–H | 278.3 | 139.8 |
| | | O2–H | 278.3 | 127.6 |

enzyme, *LE*, *BEI,* and *LLE* were evaluated. As described for drugs used as therapy, *LE* should be greater than 0.3; *BEI* should be between 20 and 27; and *LLE* between 5 and 7. As shown in Table 5, the compounds methylatrarate, methylhaeatommate, sphaeroforin, diffractaic acid, barbatolic acid, salazinic acid show a ligand efficiency greater than 0.3, consistent with a high affinity for CYP2C9*2. The affinity of the compounds methylatrarate and methylhaeatommate for CYP2C9*2 with a *BEI* value greater than 20, could show a high affinity for the enzyme. Given the amount of hydroxyl groups, the analyzed compounds *LEE* values less than 5, except for salazinic acid. However, as discussed, the *LE* and BEI values indicate that the tested compounds could bind to CYP2C9*2 which would allow to modify its activity or to be processed into compounds with different activity (see Table 6).

To assess possible non-covalent interactions, NCI calculations were performed. As shown in Fig. 7 and Figs. S8–S15, lichen compounds exhibit weak interactions with CYP2C9*2 through hydrophobic or polar residues. The possible strong interactions, such as hydrogen bonds, of residues Leu362 with methylatrarate (Fig. 7) or Arg108 with sphaeroforin (Fig. S11) are *highlighted*. Less specific interactions, given that the peptide bond participates, are those that are observed between residues Gly296 with diffractaic acid (Fig. S13), and Leu208 with lobaric acid (Fig. S9) or Sphaeroforin (Fig. S11).

## 4. Conclusions

The cyclic voltamperograms experiments showed that as the pH increases, all lichenic molecules' reduction potentials are moving to lower negative values, demonstrating that the oxidation involved $H^+$ protons. The compounds 1–4 presented slopes close to the Nernst constant, 0.059/pH, indicating a $2H^+/2e^-$ relation between protons and

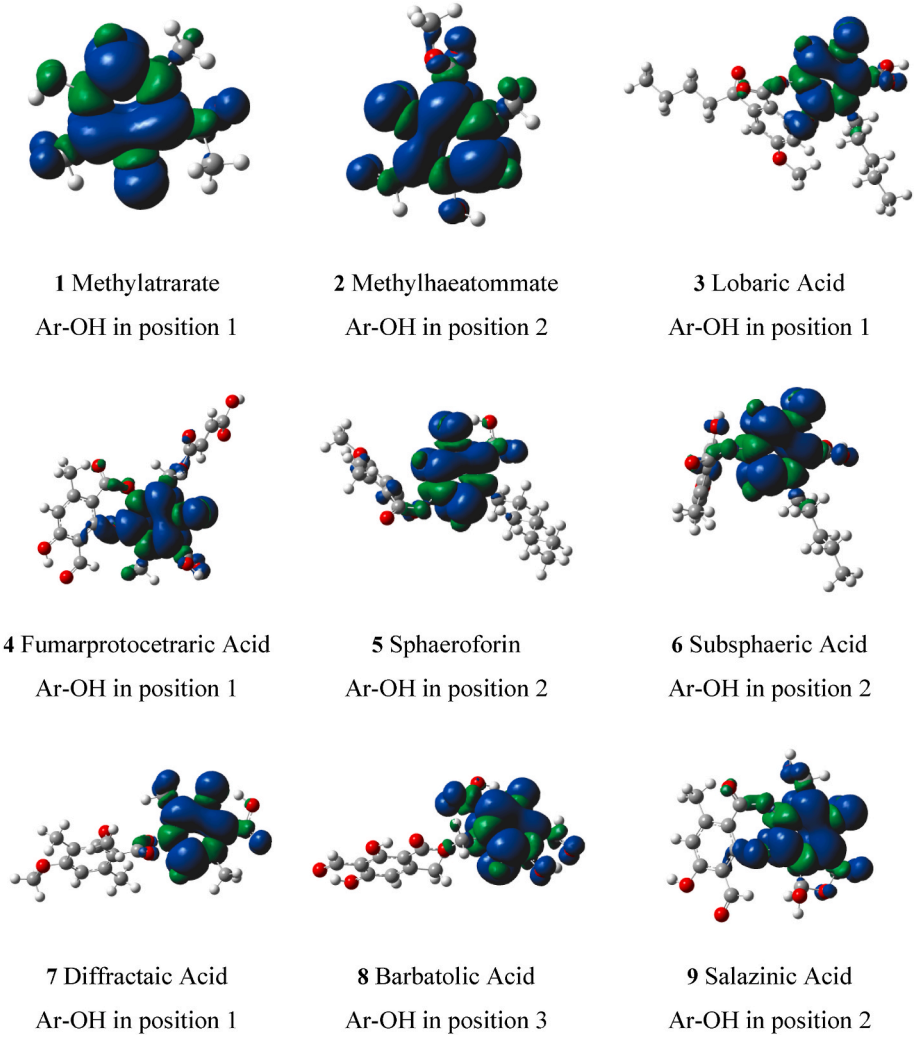


**Fig. 4.** Spin density surfaces for the lichen molecules at the second step of the sequential proton loss electron transfer (SPLET) mechanism.

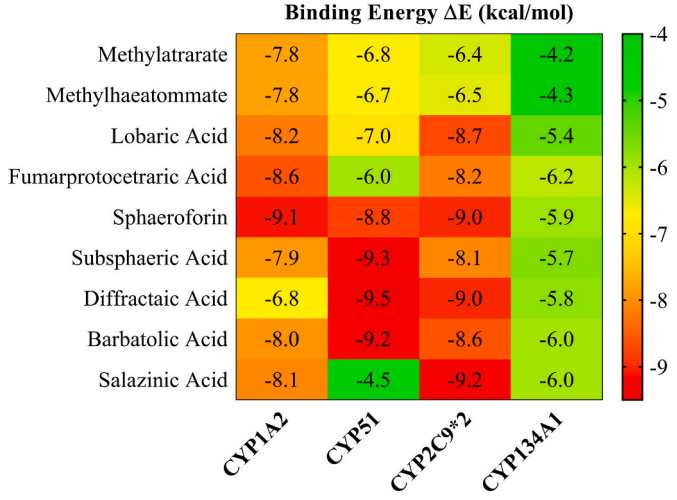


**Fig. 5.** Heatmap of the intermolecular docking energy values (kcal·mol$^{-1}$) of lichen molecules.

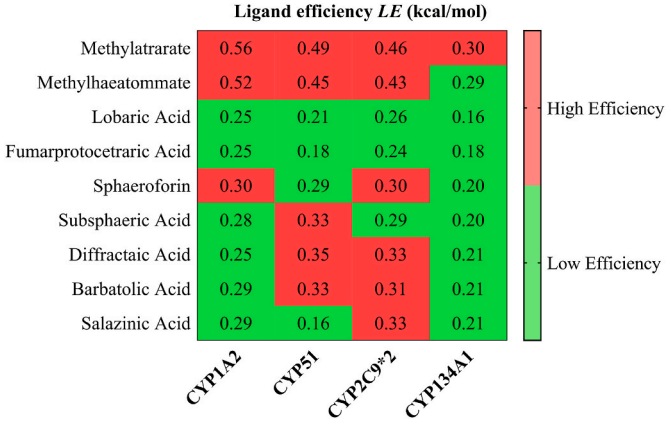


**Fig. 6.** Binary heatmap of the intermolecular docking energy values (kcal·mol$^{-1}$) of lichen molecules.

electrons, while the 5–9 systems with slopes between 0.037 and 0.032/pH indicated a $1H^{+}/2e^{-}$ link between protons and electrons. Those results show the shift of less positive potential values with the increase of pH can improve the antioxidant activity of these substances because they require less energy to oxidize. The HAT and SPLET mechanisms showed that the best antioxidant activity is exhibit by molecules with a carboxylic acid group close to a phenolic hydroxyl group: 3, 4, 5, 6, 7, and 8. The computational simulations suggest that radical stability is favored by intramolecular hydrogen bonds formed between the phenolic

**Table 5**
Molecular docking results for lichen molecules in the CYP2C9*2. Intermolecular docking energy values ($\Delta E_{binding}$), $K_d$ values, Ligand Efficiency (*LE*), Binding Efficiency Index (*BEI*), and Lipophilic Ligand Efficiency (*LLE*) for the CYP2C9*2 complexes.

| Docking and Ligand Efficiency Analysis | | | | | |
|---|---|---|---|---|---|
| Compound | $\Delta E_{binding}$ (kcal·mol$^{-1}$) | $K_d$ | *LE* (kcal·mol$^{-1}$) | *BEI* (kDa) | *LLE* |
| CYP2C9*2 | | | | | |
| Methylatrarate | −6.40 | 2.04 × 10$^{-5}$ | 0.46 | 23.91 | 3.19 |
| Methylhaeatommate | −6.50 | 1.72 × 10$^{-5}$ | 0.43 | 22.66 | 3.76 |
| Lobaric acid | −8.70 | 4.21 × 10$^{-7}$ | 0.26 | 13.97 | 0.85 |
| Fumarprotocetraric acid | −8.20 | 9.78 × 10$^{-7}$ | 0.24 | 12.72 | 3.78 |
| Sphaeroforin | −9.00 | 2.54 × 10$^{-7}$ | 0.30 | 15.84 | 1.75 |
| Subsphaeric acid | −8.10 | 1.16 × 10$^{-6}$ | 0.29 | 15.28 | 1.87 |
| Diffractaic acid | −9.00 | 2.54 × 10$^{-7}$ | 0.33 | 17.62 | 3.04 |
| Barbatolic acid | −8.60 | 4.98 × 10$^{-7}$ | 0.31 | 16.15 | 4.81 |
| Salazinic acid | −9.20 | 1.81 × 10$^{-7}$ | 0.33 | 17.36 | 5.55 |

hydroxyl groups and the hydrogen of the carboxylic acid group. Finally, the experimental conditions used for cyclic voltammetry revealed that as the pH increases a declining in the redox potentials to lower negative values are presented. According to these conditions, the anionic forms are preferred, and the SPLET mechanism could be the most appropriate scheme for study the antioxidant behaviour of the lichens substances. The lichen substances could generate an antioxidant effect mediated by interaction with CYPs enzymes, mainly CYP1A2, CYP51 and CYP2C9*2 isoforms.

## Funding

O.G.-B. Thank funding from the Ministry of Science, Technology and Innovation, the Ministry of Education, the Ministry of Industry, Commerce and Tourism, and ICETEX, Programme Ecosistema Científico-Colombia Científica, from the Francisco José de Caldas Fund, Grand RCFP44842-212-2018. CA and MS are grateful to INACH RT 16–17 and FONDECYT REGULAR N° 1190314 for supporting this work.

## Author contributions

OY, CA, WT and OG-B contributed to the conception and design of the study; CA and MS collected the lichens. CA and GC isolated the compounds 1–9. EN and C.G performed the electrochemical experiments, EO, OY and WT preformed the theoretical calculations; EO, OY and MIO organized the database; OY and MIO performed theoretical modelling with enzymes; OG-B, CA, CG and EO wrote the first draft of the manuscript; OY, OG, CA, EO and LR wrote sections of the manuscript. All authors contributed to manuscript revision, read and approved the submitted version.

**Table 6**
Amino acid residues of CYP2C9*2 protein and hydrogen bonding with the lichen molecules within a distance of 3.5 Å.

| Interacting Amino Acids in the Binding pocket of CYP2C9*2 | | |
|---|---|---|
| Compound | Amino Acids | H-bonds (Å) |
| Methylatrarate | Thr301, Ile205, Val113, Ala297, Leu362, Leu366, Heme | Thr301:OG1–Lig:O (2.73) |
| Methylhaeatommate | Ala297, Thr301, Gly296, Ala297, Ile205, Heme | Ala297:N–Lig:O (3.14) Thr301:OG1–Lig:O (3.00) |
| Lobaric acid | Arg108, Heme, Ala297, Gly296, Leu201, Ile205, Leu208, Leu233, Val237, Val113, Leu366 | Arg108:NH1–Lig:O (2.86) Arg108:NH1–Lig:O (2.83) |
| Fumarprotocetraric acid | Arg108, Val292, Phe476, Heme, Ala297, Gly296, Val113, Ile205, Leu361, Leu362, Phe114 | Arg108:NH1–Lig:O (2.81) Arg108:NH2–Lig:O (2.73) |
| Sphaeroforin | Ala103, Arg108, Phe114, Val113, Ala297, Leu208, Leu233, Val237, Leu102, Leu362, Leu366, Heme, Ala106 | Ala103:N–Lig:O (3.15) Arg108:NH1–Lig:O (2.88) |
| Subsphaeric acid | Thr301, Gly296, Ala106, Leu233, Phe114, Phe476, Ala297, Val237 | Thr301:OG1–Lig:H (2.50) Gly296:CA–Lig:O (3.35) |
| Diffractaic acid | Ala297, Phe476, Phe114, Gly296, Ala106, Arg108, Val237, Leu201, Ile205, Leu362, Leu366, Val113, Leu208 | Ala297:N–Lig:O (3.10) |
| Barbatolic acid | Arg108, Ala297, Phe114, Val113, Leu366, Leu208 | Arg108:NH1–Lig:O (3.17) Ala297:N–Lig:O (3.05) |
| Salazinic acid | Arg108, Leu201, Asp293, Phe476, Heme, Gly296, Ala297, Ile205, Leu361, Leu362 | Arg108:NH2–Lig:O (3.33) Leu201:O–Lig:H (2.22) Asp293:CA–Lig:O (3.40) Asp293:O–Lig:O (2.87) |

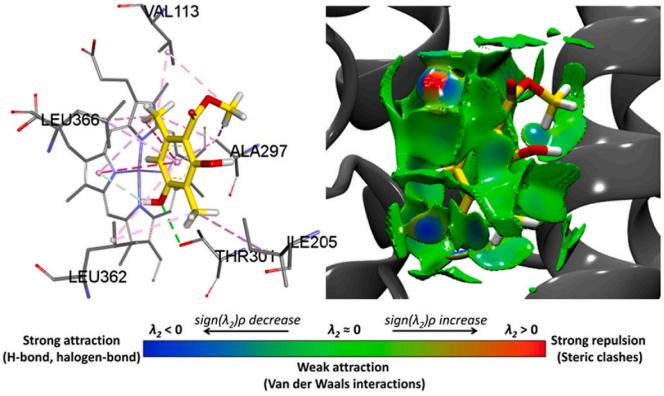


**Fig. 7.** Docking and NCI analysis for Methylatrarate bound to CYP2C9*2. The surrounding amino acid residues in the binding pocket of CYP2C9*2 within 3.0 Å. The reason of 3.0 Å was the length of the hydrogen bond ranges from 2.6 Å to 3.1 Å based on observation from the PDB.

## Declaration of competing interest

The authors declare that they have no known competing financial interests or personal relationships that could have appeared to influence the work reported in this paper.

## Data availability

Data will be made available on request.

## Acknowledgments

O.G.-B. Thank funding from the Ministry of Science, Technology, and Innovation, the Ministry of Education, the Ministry of Industry, Commerce and Tourism, and ICETEX, Programme Ecosistema Científico-Colombia Científica, from the Francisco José de Caldas Fund, Grand RCFP44842-212-2018.

## Appendix A. Supplementary data

Supplementary data to this article can be found online at https://doi.org/10.1016/j.cbi.2023.110357.

## References

[1] V. Kagan, E. Serbinova, K. Novikov, V. Ritov, Y. Kozlov, T. Stoytchev, Toxic and protective effects of antioxidants in biomembranes, Arch. Toxicol. 59 (1986) 302–305, https://doi.org/10.1007/978-3-642-71248-7_51.
[2] P.A.S. White, R.C.M. Oliveira, A.P. Oliveira, M.R. Serafini, A.A.S. Araújo, D. P. Gelain, J.C.F. Moreira, J.R.G.S. Almeida, J.S.S. Quintans, L.J. Quintans-Junior, M.R.V. Santos, Antioxidant activity and mechanisms of action of natural compounds isolated from lichens: a systematic review, Molecules 19 (2014) 14496–14527, https://doi.org/10.3390/molecules190914496.
[3] J.M. McCord, The evolution of free radicals and oxidative stress, Am. J. Med. 108 (2000) 652–659, https://doi.org/10.1016/S0002-9343(00)00412-5.
[4] C. Trautwein, S.L. Friedman, D. Schuppan, M. Pinzani, Hepatic fibrosis: concept to treatment, J. Hepatol. 62 (2015) S15–S24, https://doi.org/10.1016/j.jhep.2015.02.039.
[5] A. Torres-Benítez, M. Rivera-Montalvo, B. Sepúlveda, O.N. Castro, E. Nagles, M. J. Simirgiotis, O. Garciá-Beltrán, C. Areche, Metabolomic analysis of two parmotrema lichens: P. Robustum (Degel.) hale and P. Andinum (mull. Rg.) hale using UHPLC-ESI-OT-MS-MS, Molecules (2017), https://doi.org/10.3390/molecules22111861.
[6] J. Boustie, S. Tomasi, M. Grube, Bioactive lichen metabolites: alpine habitats as an untapped source, Phytochemistry Rev. 10 (2011) 287–307, https://doi.org/10.1007/s11101-010-9201-1.
[7] I. Gülçin, M. Oktay, Ö.I. Küfrevioğlu, A. Aslan, Determination of antioxidant activity of lichen Cetraria islandica (L) Ach, J. Ethnopharmacol. 79 (2002) 325–329, https://doi.org/10.1016/S0378-8741(01)00396-8.
[8] M. Kosanić, B. Ranković, Lichens as possible sources of antioxidants, Pak. J. Pharm. Sci. 24 (2011) 165–170.
[9] B. Paudel, H.D. Bhattarai, D.P. Pandey, J.S. Hur, S.G. Hong, I.C. Kim, J.H. Yim, Antioxidant, antibacterial activity and brine shrimp toxicity test of some mountainous lichens from Nepal, Biol. Res. 45 (2012) 387–391, https://doi.org/10.4067/S0716-97602012000400010.
[10] B. Ranković, M. Kosanić, N. Manojlović, A. Rančić, T. Stanojković, Chemical composition of Hypogymnia physodes lichen and biological activities of some its major metabolites, Med. Chem. Res. 23 (2014) 408–416, https://doi.org/10.1007/s00044-013-0644-y.
[11] M. Kosanić, N. Manojlović, S. Janković, T. Stanojković, B. Ranković, Evernia prunastri and Pseudoevernia furfuraceae lichens and their major metabolites as antioxidant, antimicrobial and anticancer agents, Food Chem. Toxicol. 53 (2013) 112–118, https://doi.org/10.1016/j.fct.2012.11.034.
[12] F. Salgado, L. Albornoz, C. Cortéz, E. Stashenko, K. Urrea-Vallejo, E. Nagles, C. Galicia-Virviescas, A. Cornejo, A. Ardiles, M. Simirgiotis, O. García-Beltrán, C. Areche, Secondary metabolite profiling of species of the genus usnea by UHPLC-ESI-OT-MS-MS, Molecules (2018), https://doi.org/10.3390/molecules23010054.
[13] V. Shukla, G.P. Joshi, M.S.M. Rawat, Lichens as a potential natural source of bioactive compounds: a review, Phytochemistry Rev. 9 (2010) 303–314, https://doi.org/10.1007/s11101-010-9189-6.
[14] C. Areche, J.R. Parra, B. Sepulveda, O. García-Beltrán, M.J. Simirgiotis, UHPLC-MS metabolomic fingerprinting, antioxidant, and enzyme inhibition activities of Himantormia lugubris from Antarctica, Metabolites 12 (2022) 560, https://doi.org/10.3390/metabo12060560.
[15] V.B. Tatipamula, S.S.P. Annam, Antimycobacterial activity of acetone extract and isolated metabolites from folklore medicinal lichen Usnea laevis Nyl. against drug-sensitive and multidrug-resistant tuberculosis strains, J. Ethnopharmacol. 282 (2022), 114641, https://doi.org/10.1016/j.jep.2021.114641.
[16] L. Fagnani, L. Nazzicone, P. Bellio, N. Franceschini, D. Tondi, A. Verri, S. Petricca, R. Iorio, G. Amicosante, M. Perilli, G. Celenza, Protocetraric and salazinic acids as potential inhibitors of SARS-CoV-2 3CL Protease: biochemical, cytotoxic, and computational characterization of depsidones as slow-binding inactivators, Pharmaceuticals 15 (2022) 714, https://doi.org/10.3390/ph15060714.
[17] A. Kocovic, J. Jeremic, J. Bradic, M. Sovrlic, J. Tomovic, P. Vasiljevic, M. Andjic, N. Draginic, M. Grujovic, K. Mladenovic, D. Baskic, S. Popovic, S. Matic, V. Zivkovic, N. Jeremic, V. Jakovljevic, N. Manojlovic, Phytochemical analysis, antioxidant, antimicrobial, and cytotoxic activity of different extracts of xanthoparmelia stenophylla lichen from stara planina, Serbia, Plants 11 (2022) 1624, https://doi.org/10.3390/plants11131624.
[18] T.K. Kim, J.M. Hong, K.H. Kim, S.J. Han, I.C. Kim, H. Oh, J.H. Yim, Potential of ramalin and its derivatives for the treatment of alzheimer's disease, Molecules 26 (2021) 1–12, https://doi.org/10.3390/molecules26216445.
[19] K. Molnár, E. Farkas, Current results on biological activities of lichen secondary metabolites: a review, Zeitschrift Fur Naturforsch. - Sect. C J. Biosci. 65 (2010) 157–173, https://doi.org/10.1515/znc-2010-3-401.
[20] A.S. Nugraha, L.F. Untari, A. Laub, A. Porzel, K. Franke, L.A. Wessjohann, Anthelmintic and antimicrobial activities of three new depsides and ten known depsides and phenols from Indonesian lichen: parmelia cetrata Ach, Nat. Prod. Res. 35 (2021) 5001–5010, https://doi.org/10.1080/14786419.2020.1761361.
[21] T.H. Do, T.H. Duong, H.T. Nguyen, T.H. Nguyen, J. Sichaem, C.H. Nguyen, H. H. Nguyen, N.P. Long, Article biological activities of lichen-derived monoaromatic compounds, Molecules 27 (2022), https://doi.org/10.3390/molecules27092871.
[22] M.S. Brewer, Natural antioxidants: sources, compounds, mechanisms of action, and potential applications, Compr. Rev. Food Sci. Food Saf. 10 (2011) 221–247, https://doi.org/10.1111/j.1541-4337.2011.00156.x.
[23] E. Osorio, J.K. Olson, W. Tiznado, A.I. Boldyrev, Analysis of why boron avoids sp 2 hybridization and classical structures in the B nH n+2 series, Chem. Eur J. 18 (2012) 9677–9681, https://doi.org/10.1002/chem.201200506.
[24] G.W. Burton, T. Doba, E. Gabe, L. Hughes, F.L. Lee, L. Prasad, K.U. Ingold, Autoxidation of biological molecules. 4. Maximizing the antioxidant activity of phenols, J. Am. Chem. Soc. 107 (1985) 7053–7065, https://doi.org/10.1021/ja00310a049.
[25] M.C. Foti, C. Daquino, C. Geraci, Electron-transfer reaction of cinnamic acids and their methyl esters with the DPPH. Radical in alcoholic solutions, J. Org. Chem. 69 (2004) 2309–2314, https://doi.org/10.1021/jo035758q.
[26] C. Areche, B.K. Cassels, W. Tiznado, Structure – Antioxidant Activity Relationships in Boldine and Glaucine : a DFT Study †, 2021, pp. 590–596, https://doi.org/10.1039/d0nj04028b.
[27] A. Vásquez-Espinal, O. Yañez, E. Osorio, C. Areche, O. García-Beltrán, L.M. Ruiz, B. K. Cassels, W. Tiznado, Theoretical study of the antioxidant activity of quercetin oxidation products, Front. Chem. 7 (2019), https://doi.org/10.3389/fchem.2019.00818.
[28] E. Osorio, E.G. Pérez, C. Areche, L.M. Ruiz, B.K. Cassels, E. Flórez, Why Is Quercetin a Better Antioxidant than Taxifolin ? Theoretical Study of Mechanisms Involving Activated Forms, 2013, pp. 2165–2172, https://doi.org/10.1007/s00894-012-1732-5.
[29] F. Salgado, J. Caballero, R. Vargas, A. Cornejo, C. Areche, Continental and Antarctic Lichens: isolation, identification and molecular modeling of the depside tenuiorin from the Antarctic lichen Umbilicaria Antarctica as tau protein inhibitor, Nat. Prod. Res. 34 (2020) 646–650, https://doi.org/10.1080/14786419.2018.1492576.
[30] C. González, C. Cartagena, L. Caballero, F. Melo, C. Areche, A. Cornejo, The fumarprotocetraric acid inhibits tau covalently, avoiding cytotoxicity of aggregates in cells, Molecules 26 (2021) 1–11, https://doi.org/10.3390/molecules26123760.
[31] T.K. Shameera Ahamed, V.K. Rajan, K. Sabira, K. Muraleedharan, DFT and QTAIM based investigation on the structure and antioxidant behavior of lichen substances Atranorin, Evernic acid and Diffractaic acid, Comput. Biol. Chem. 80 (2019) 66–78, https://doi.org/10.1016/j.compbiolchem.2019.03.009.
[32] R. Krishnan, J.S. Binkley, R. Seeger, J.A. Pople, Self-consistent molecular orbital methods. XX. A basis set for correlated wave functions, J. Chem. Phys. 72 (1980) 650–654, https://doi.org/10.1063/1.438955.
[33] A.D. McLean, G.S. Chandler, Contracted Gaussian basis sets for molecular calculations. I. Second row atoms, Z=11-18, J. Chem. Phys. 72 (1980) 5639–5648, https://doi.org/10.1063/1.438980.
[34] M.J. Frisch, G.W. Trucks, H.E. Schlegel, G.E. Scuseria, M.A. Robb, J.R. Cheeseman, G. Scalmani, V. Barone, G.A. Petersson, F. O, J.B. Foresman, J.D. Fox, Gaussian 16, Gaussian, Inc., Wallingford CT, 2016.
[35] S.V. Jovanovic, S. Steenken, M. Tosic, B. Marjanovic, M.G. Simic, Flavonoids as antioxidants, J. Am. Chem. Soc. 116 (1994) 4846–4851, https://doi.org/10.1021/ja00090a032.
[36] J.E. Bartmess, Thermodynamics of the electron and the proton, J. Phys. Chem. 98 (1994) 6420–6424, https://doi.org/10.1021/j100076a029.
[37] S. Sansen, J.K. Yano, R.L. Reynald, G.A. Schoch, K.J. Griffin, C.D. Stout, E. F. Johnson, Adaptations for the oxidation of polycyclic aromatic hydrocarbons exhibited by the structure of human P450 1A2, J. Biol. Chem. 282 (2007) 14348–14355, https://doi.org/10.1074/jbc.M611692200.
[38] T.Y. Hargrove, L. Friggeri, Z. Wawrzak, A. Qi, W.J. Hoekstra, R.J. Schotzinger, J. D. York, F. Peter Guengerich, G.I. Lepesheva, Structural analyses of Candida albicans sterol 14α-demethylase complexed with azole drugs address the molecular basis of azole-mediated inhibition of fungal sterol biosynthesis, J. Biol. Chem. 292 (2017) 6728–6743, https://doi.org/10.1074/jbc.M117.778308.
[39] S.J. Parikh, C.M. Evans, J.O. Obi, Q. Zhang, K. Maekawa, K.C. Glass, M.B. Shah, Structure of cytochrome P450 2C9*2 in complex with losartan: insights into the effect of genetic polymorphism, Mol. Pharmacol. 98 (2020) 529–539, https://doi.org/10.1124/MOLPHARM.120.000042.
[40] RCSB PDB - 7OW9, Crystal structure of a staphylococcal orthologue of CYP134A1 (CYPX) in complex with Cyclo-L-leucyl-L-leucine (n.d.), https://www.rcsb.org/structure/7OW9. (Accessed 31 January 2022).
[41] H.M. Berman, J. Westbrook, Z. Feng, G. Gilliland, T.N. Bhat, H. Weissig, I. N. Shindyalov, P.E. Bourne, The protein Data Bank, Nucleic Acids Res. 28 (2000) 235–242, https://doi.org/10.1093/nar/28.1.235.

[42] O. Trott, A. Olson, AutoDock Vina, Improving the speed and accuracy of docking with a new scoring function, efficient optimization and multithreading, J. Comput. Chem. 31 (2010) 455–461, https://doi.org/10.1002/jcc.21334.
[43] J.J.P. Stewart, MOPAC, 2016.
[44] J.J.P. Stewart, Optimization of parameters for semiempirical methods V: modification of NDDO approximations and application to 70 elements, J. Mol. Model. 13 (2007) 1173–1213, https://doi.org/10.1007/s00894-007-0233-4.
[45] J. Řezáč, P. Hobza, Advanced corrections of hydrogen bonding and dispersion for semiempirical quantum mechanical methods, J. Chem. Theor. Comput. 8 (2012) 141–151, https://doi.org/10.1021/ct200751e.
[46] M. Banck, T. Vandermeersch, N.M. O'Boyle, G.R. Hutchison, C. Morley, C. A. James, Open Babel, An open chemical toolbox, J. Cheminf. 3 (2011) 33, https://doi.org/10.1186/1758-2946-3-33.
[47] G. Madhavi Sastry, M. Adzhigirey, T. Day, R. Annabhimoju, W. Sherman, Protein and ligand preparation: parameters, protocols, and influence on virtual screening enrichments, J. Comput. Aided Mol. Des. 27 (2013) 221–234, https://doi.org/10.1007/s10822-013-9644-8.
[48] G.M. Morris, D.S. Goodsell, R.S. Halliday, R. Huey, W.E. Hart, R.K. Belew, A. J. Olson, Automated docking using a Lamarckian genetic algorithm and an empirical binding free energy function, J. Comput. Chem. 19 (1998) 1639–1662, https://doi.org/10.1002/(SICI)1096-987X(19981115)19:14<1639::AID-JCC10>3.0.CO;2-B.
[49] Dassault Systèmes BIOVIA, Discovery Studio Modeling Environment, 2017.
[50] E.R. Johnson, S. Keinan, P. Mori-Sánchez, J. Contreras-García, A.J. Cohen, W. Yang, Revealing noncovalent interactions, J. Am. Chem. Soc. 132 (2010) 6498–6506, https://doi.org/10.1021/ja100936w.
[51] J. Contreras-García, E.R. Johnson, S. Keinan, R. Chaudret, J.-P. Piquemal, D. N. Beratan, W. Yang, NCIPLOT: a program for plotting noncovalent interaction regions, J. Chem. Theor. Comput. 7 (2011) 625–632, https://doi.org/10.1021/ct100641a.
[52] W. Humphrey, A. Dalke, K. Schulten, VMD: visual molecular dynamics, J. Mol. Graph. 14 (1996) 33–38, https://doi.org/10.1016/0263-7855(96)00018-5.
[53] C. Abad-Zapatero, Ligand efficiency indices for effective drug discovery, Expet Opin. Drug Discov. 2 (2007) 469–488, https://doi.org/10.1517/17460441.2.4.469.
[54] C. Abad-Zapatero, O. Perišić, J. Wass, A.P. Bento, J. Overington, B. Al-Lazikani, M. E. Johnson, Ligand efficiency indices for an effective mapping of chemico-biological space: the concept of an atlas-like representation, Drug Discov. Today 15 (2010) 804–811, https://doi.org/10.1016/J.DRUDIS.2010.08.004.
[55] C. Abad-Zapatero, Ligand Efficiency Indices for Drug Discovery, Academic Press, San Diego, 2013, https://doi.org/10.1016/B978-0-12-404635-1.00009-8.
[56] C.H. Reynolds, B.A. Tounge, S.D. Bembenek, Ligand binding efficiency: trends, physical basis, and implications, J. Med. Chem. 51 (2008) 2432–2438, https://doi.org/10.1021/jm701255b.
[57] M.M. Cavalluzzi, G.F. Mangiatordi, O. Nicolotti, G. Lentini, Ligand efficiency metrics in drug discovery: the pros and cons from a practical perspective, Expet Opin. Drug Discov. 12 (2017) 1087–1104, https://doi.org/10.1080/17460441.2017.1365056.
[58] D.F. Veber, S.R. Johnson, H.-Y. Cheng, B.R. Smith, K.W. Ward, K.D. Kopple, Molecular properties that influence the oral bioavailability of drug candidates, J. Med. Chem. 45 (2002) 2615–2623, https://doi.org/10.1021/jm020017n.
[59] A. Daina, O. Michielin, V. Zoete, SwissADME: a free web tool to evaluate pharmacokinetics, drug-likeness and medicinal chemistry friendliness of small molecules, Sci. Rep. 7 (2017) 1–13, https://doi.org/10.1038/srep42717.
[60] A.J. Blasco, A.G. Crevillén, M.C. González, A. Escarpa, Direct electrochemical sensing and detection of natural antioxidants and antioxidant capacity in vitro systems, Electroanalysis 19 (2007) 2275–2286, https://doi.org/10.1002/elan.200704004.
[61] G. Ziyatdinova, E. Kozlova, H. Budnikov, Electropolymerized eugenol-MWNT-based electrode for voltammetric evaluation of wine antioxidant capacity, Electroanalysis 27 (2015) 1660–1668, https://doi.org/10.1002/elan.201400712.
[62] J.O. Miners, D.J. Birkett, Cytochrome P4502C9: an enzyme of major importance in human drug metabolism, Br. J. Clin. Pharmacol. 45 (1998) 525–538, https://doi.org/10.1046/j.1365-2125.1998.00721.x.